Introduction to 3D Fringe Projection Profilometry and The Optimal Frequency Selection

Tomislav Petković
tomislav.petkovic.jr@fer.hr
University of Zagreb
Faculty of Electrical Engineering and Computing

Croatian Science Foundation

Acknowledgment

- Project “Robust Structured Light Coding for 3D Imaging in Difficult Conditions” has been supported by the Croatian Science Foundation under the grant numbers HRZZ-IP-2019-04-9157 and DOK-2021-02-9474

- Webpage: https://www.fer.unizg.hr/3dcoding/en
- Project team:
  - Tomislav Petković, University of Zagreb
  - Tomislav Pribanić, University of Zagreb
  - Domagoj Zoraja, University of Zagreb
  - Simone Gasparini, INP ENSEEIHT, Tolouse, France
  - Josep Forest Collado, ViCOROB Universitat de Girona, Girona, Spain
  - Joaquim Salvi Mas, Universitat de Girona, Girona, Spain
  - Antonio Vasilijević, AURLab, Norwegian University of Science and Technology, Trondheim, Norway

Hrzz
Croatian Science Foundation

Outline

- What is 3D profilometry?
- Fringe projection profilometry
  - structured light patterns
  - fringe patterns
  - wrapped phase and phase unwrapping
  - examples
- Multi-camera multi-projector structured light scanner
  - phase unwrapping and selection of spatial frequencies
  - on geometric and colorimetric calibration (for discussion only)
- On optimal frequency selection
  - distance in wrapped phase space as fringe design criteria
  - some designed patterns
  - point-cloud filtering
- Underwater structured light imaging
  - future research directions
- Conclusion

What is 3D profilometry?

- 3D profilometry is the measurement of coordinates of selected points which are located on the surface of an object.
  - Other names: 3D surface scanning, range finding, depth sensing
  - 3D coordinates (*x*, *y*, *z*) are always measured, and sometimes surface reflectance, surface color or albedo are also measured
  - Resulting data is called a point cloud
  - Specific measurement techniques: structured light scanning, fringe projection profilometry, stereo vision, time-of-flight
  - 3D profilometry vs 3D imaging: in 3D imaging we measure some property *p* for each point (*x*, *y*, *z*) within a finite volume (e.g. CT, MRI, 3DRA)


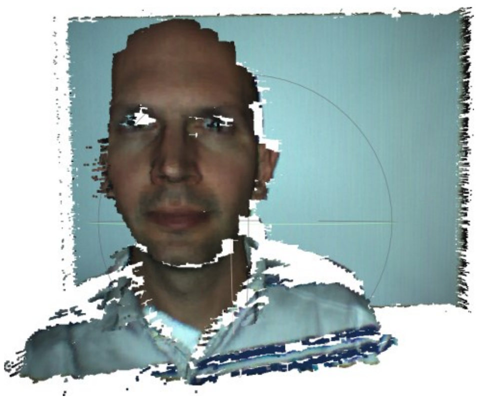


Structured light scanning

- In structured light scanning an artificial controllable light source is used to illuminate a scene
  - projectors project images
- Multiple measurements are made for various projected patterns
  - cameras acquire images of the object on which patterns are projected
- Computational imaging is used to extract the data of interest
  - decoding the projected code or observing how the pattern is deformed enables 3D measurement

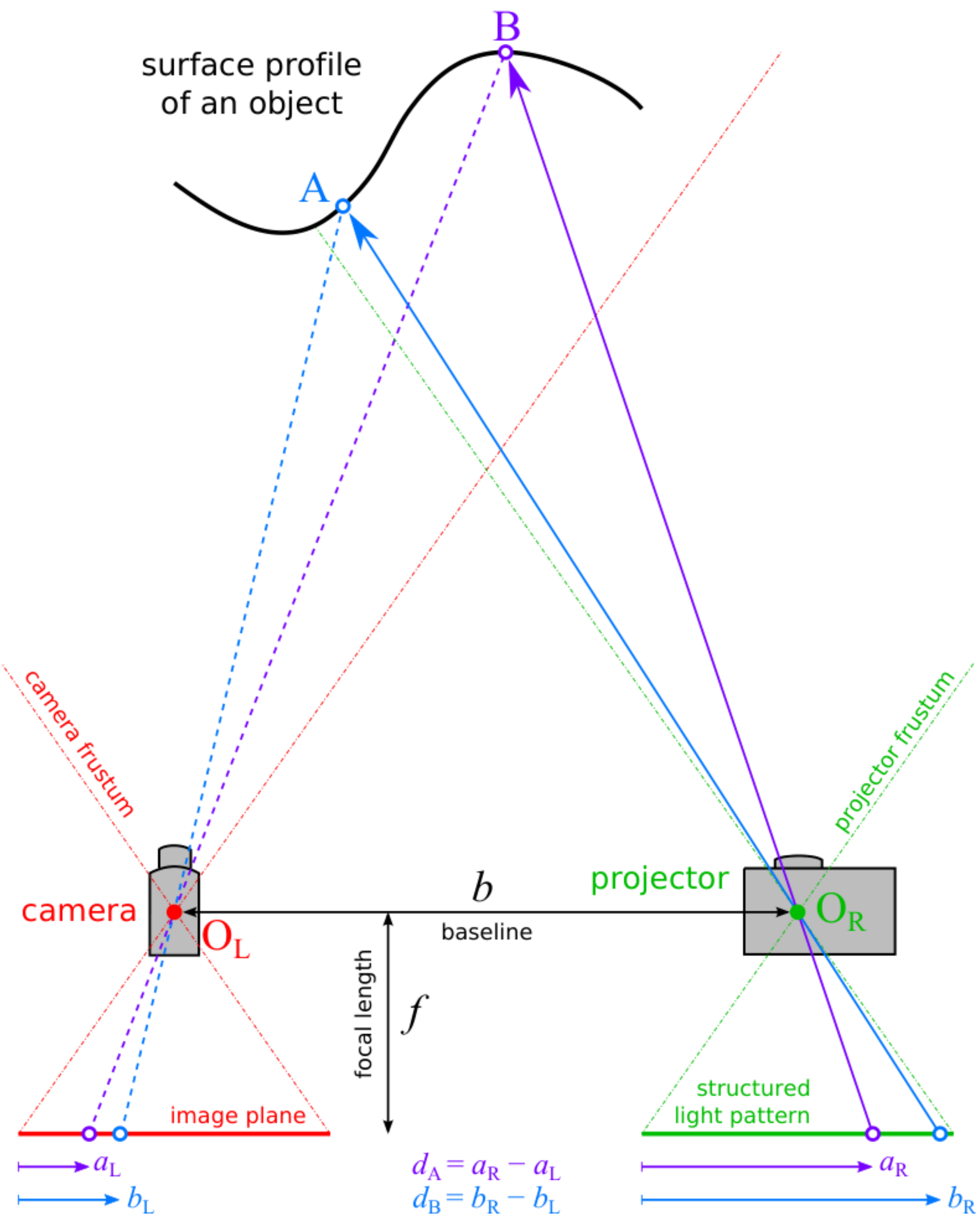

Structured Light Patterns

- In structured light surface scanning we may project one or more patterns:

1) one-shot patterns
   - reconstruction from a single image
   - object may move
   - spatial pattern decoding
   - reconstruction is usually sparse or low-resolution

2) multi-shot patterns
   - multiple images are projected in time
   - object must be stationary
   - temporal pattern decoding
   - reconstruction is dense or high-resolution

- Fringe projection profilometry: pattern is a **sinusoidal fringe**.

Examples of structured light patterns

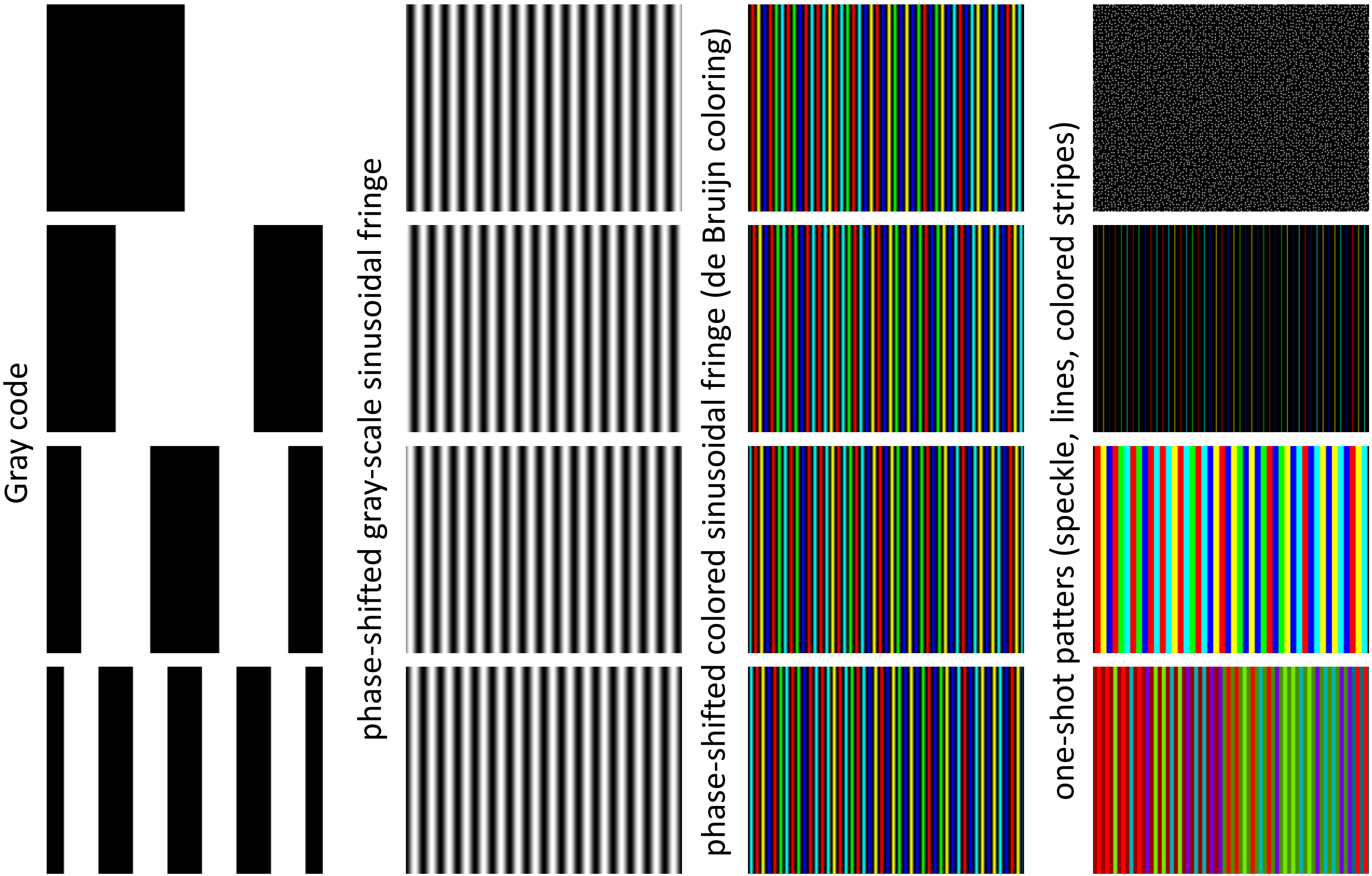

Projector-camera pair (a common setup)

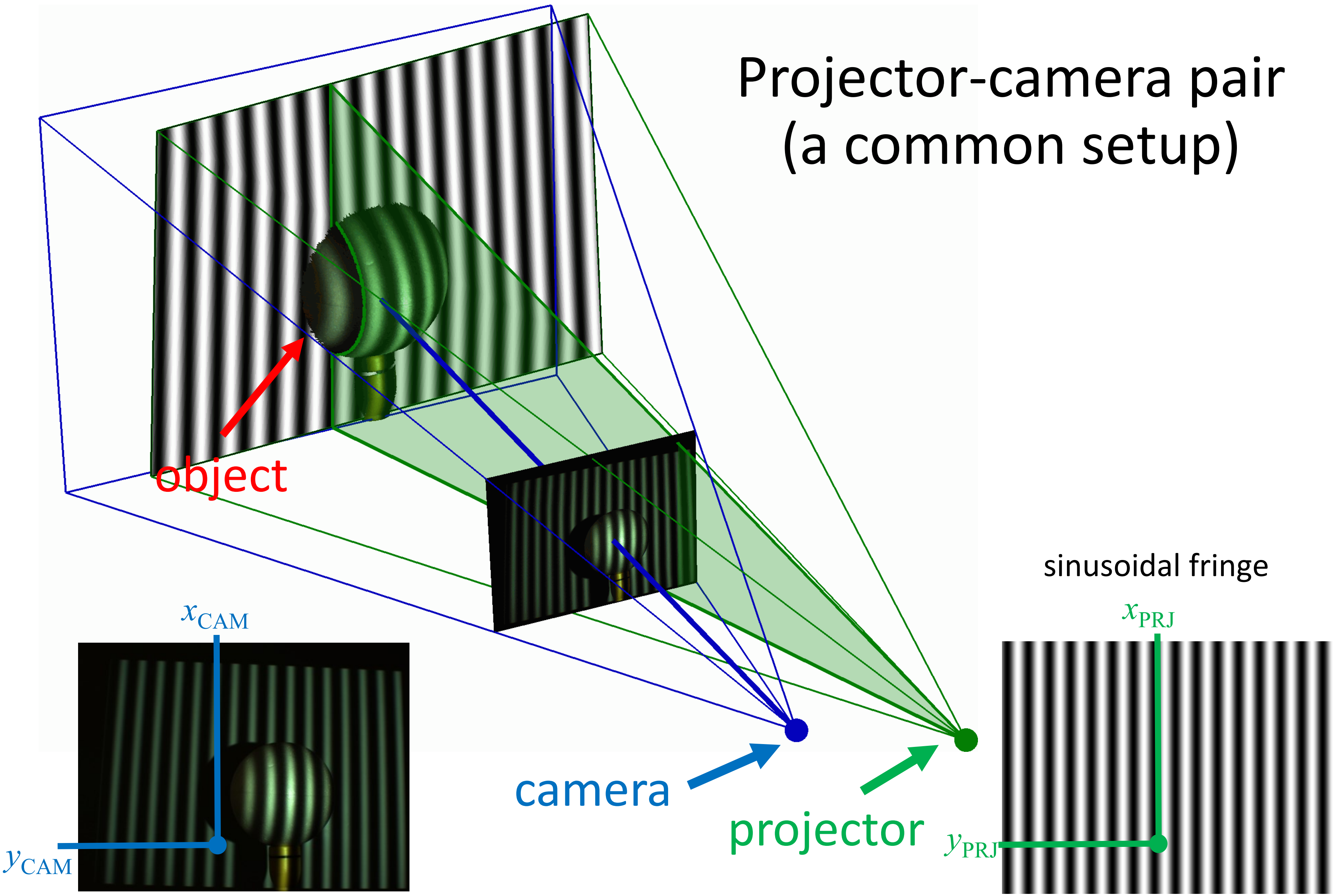

Wrapped phase and phase unwrapping

- The intensity of a sinusoidal fringe which encodes x_{PRJ} as the argument of the cosine is

$$I_{\mathrm{PRJ}}(x_{\mathrm{PRJ}}, y_{\mathrm{PRJ}}) = I_0\big(1 + \cos(\omega x_{\mathrm{PRJ}} - \varphi[n])\big)/2$$

- Projecting at least three patterns with phase shifts $\varphi[n]$ enables the recovery of ωx_{PRJ}, but only up to mod 2π
- The phase is wrapped and must be unwrapped by determining the fringe order number k

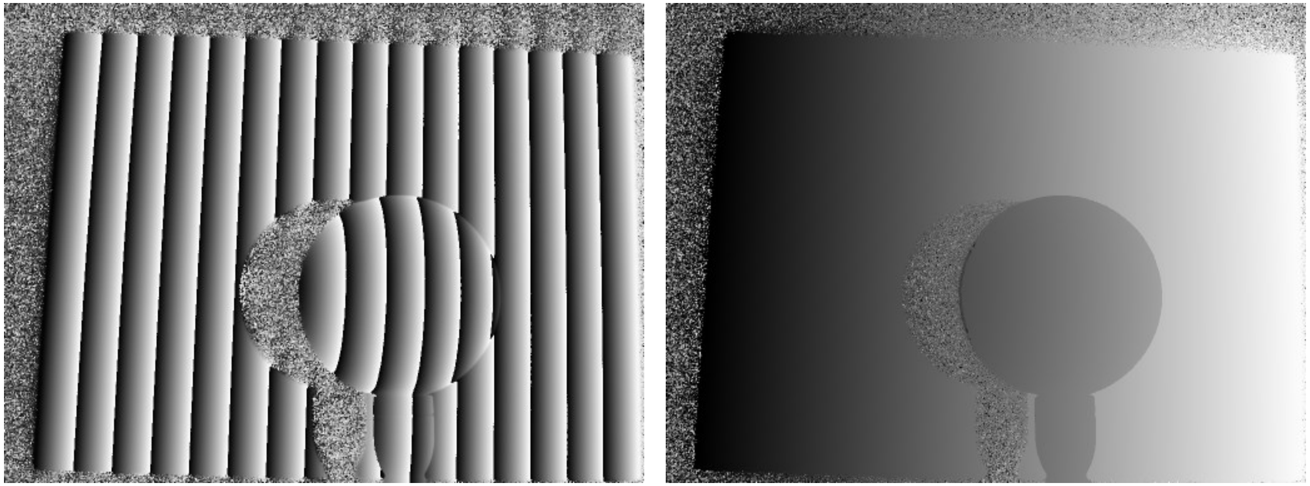

$$\Phi = \varphi + 2k\pi$$

Human body scanner

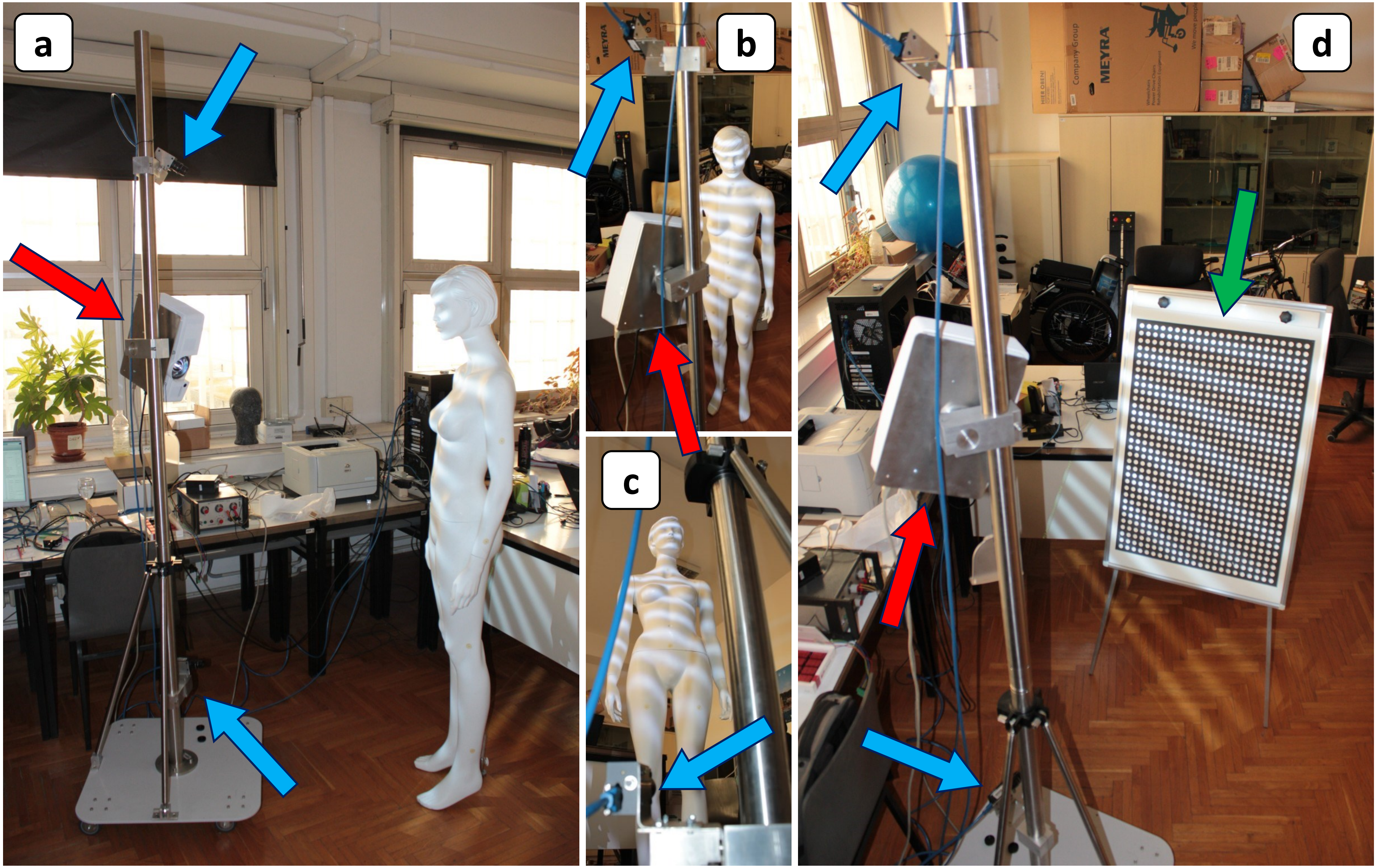

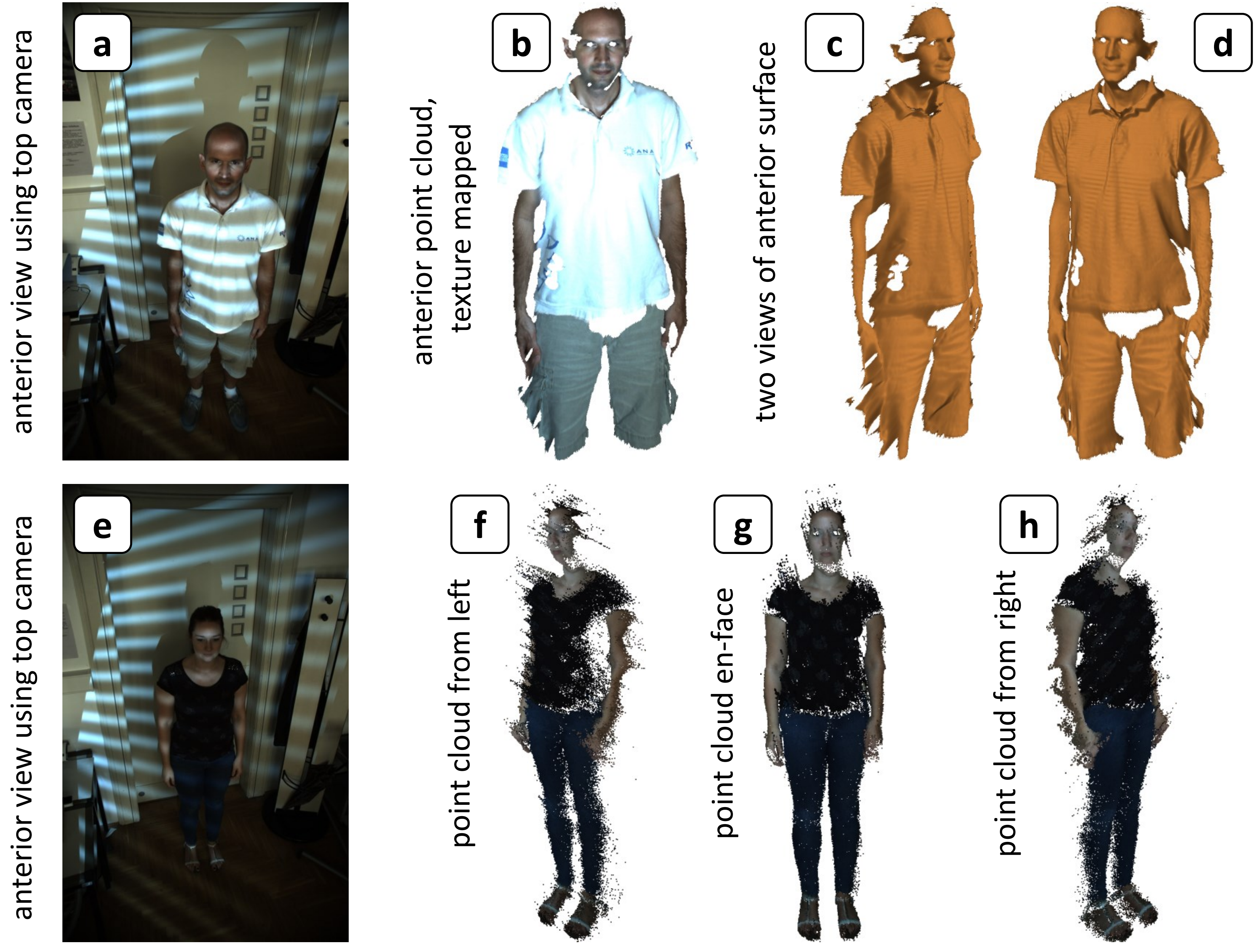
a
anterior view using top camera
b
anterior point cloud,
texture mapped
c
two views of anterior surface
d
e
anterior view using top camera
f
point cloud from left
g
point cloud en-face
h
point cloud from right

Common issues/design challenges

- Have to take into consideration: occlusions, ambient illumination, interreflections, non-Lambertian surfaces (shiny, semi-transparent, ...), etc.

- We want to measure the whole surface of an object
  - multiple measurements are usually required
  - reposition or move either the object or the measuring device
  - increase the number of sensors (increasing the number of projectors introduces interferences)

- We want to measure under normal illumination
  - dark rooms are impractical for everyday scanning
  - structured light pattern should be insensitive to ambient illumination

- We want good quality scans which require minimal post-processing
  - automatic rejection of bad measurement points

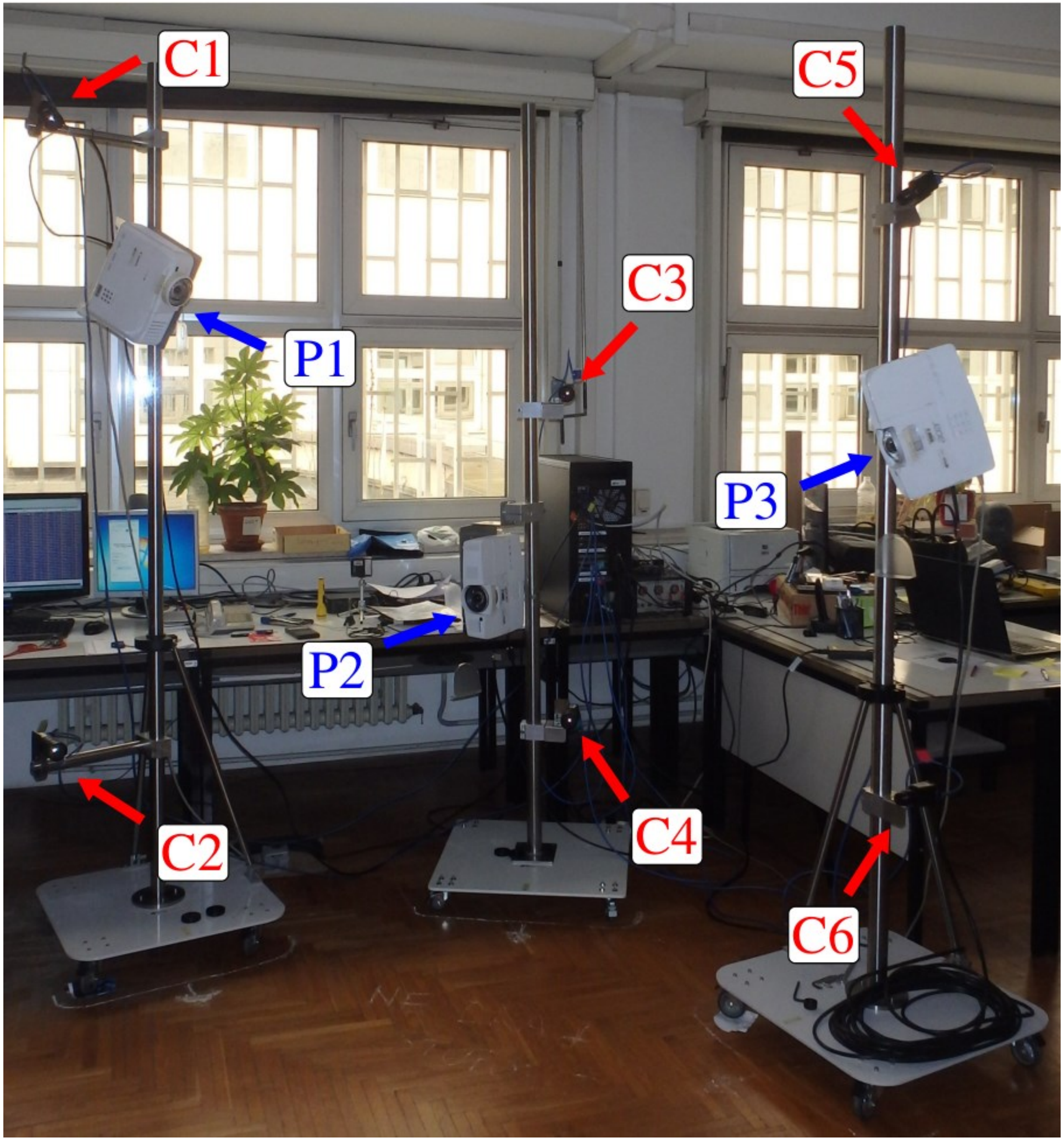

A flexible laboratory setup

- Three carts with poles
  - easy positioning
- Each pole contains
  - one projector
  - two cameras

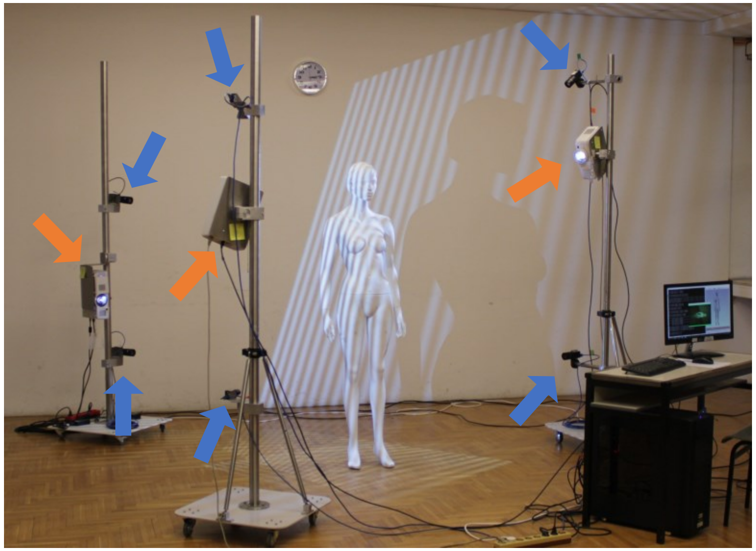
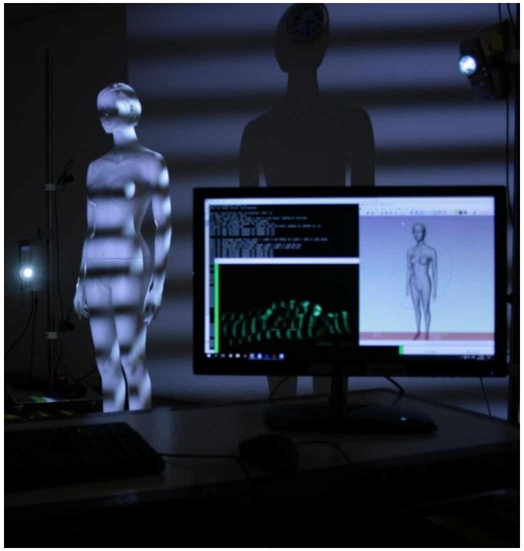



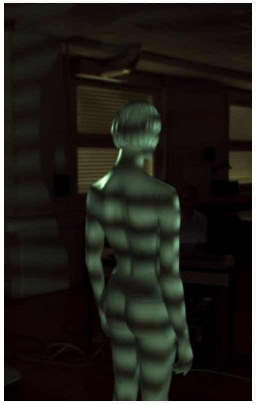

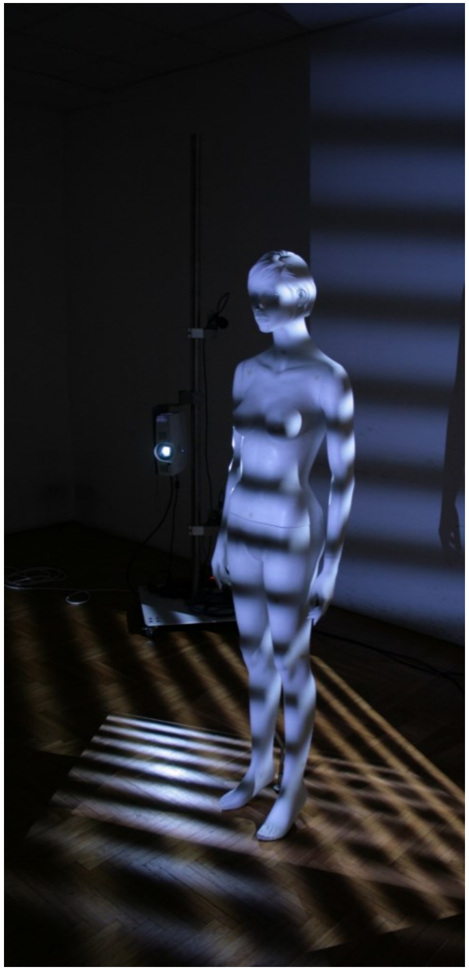
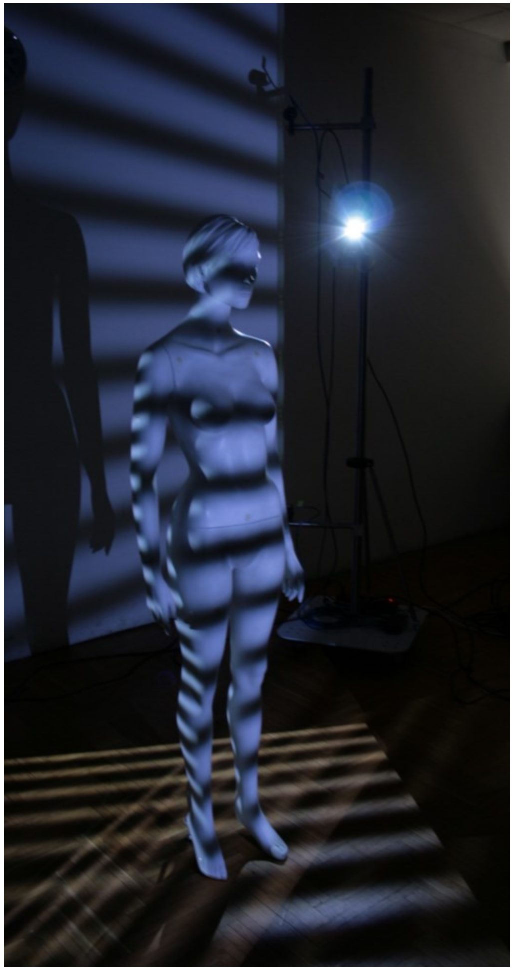

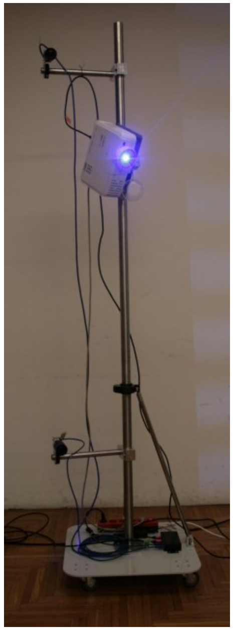

What do we project and observe?

- A projector is projecting a sinusoidal fringe

$$I_{\mathrm{PRJ}}(x_{\mathrm{PRJ}}, y_{\mathrm{PRJ}}) = I_0\big(1 + \cos(\omega x_{\mathrm{PRJ}} - \varphi[n])\big)/2$$

- A camera observing the pattern of one projector measures the intensity

$$I_{\mathrm{CAM}}(x_{\mathrm{CAM}}, y_{\mathrm{CAM}}) = I_{\mathrm{AMB}} + hI_{\mathrm{PRJ}}$$

- If multiple projectors are projecting simultaneously

$$I_{\mathrm{CAM}} = a + \sum\nolimits_{p=1}^{P} b_p \cos(\omega_p x_{\mathrm{PRJ},p} - \varphi_p[n])$$

Decomposition of the observed intensities

- Requires solving a system of linear equations:

$$I_{\mathrm{CAM}}[n] = a + \sum\nolimits_{p=1}^{P} b_p \cos(\omega_p x_{\mathrm{PRJ},p}) \cos(\varphi_p[n]) + \sum\nolimits_{p=1}^{P} b_p \sin(\omega_p x_{\mathrm{PRJ},p}) \sin(\varphi_p[n])$$

$$\mathbf{w} = \begin{bmatrix} w_0 \\ w_{c,1} \\ w_{s,1} \\ \vdots \\ w_{c,P} \\ w_{s,P} \end{bmatrix} = \begin{bmatrix} a \\ b_1 \cos(\omega_1 x_{\mathrm{PRJ},1}) \\ b_1 \sin(\omega_1 x_{\mathrm{PRJ},1}) \\ \vdots \\ b_P \cos(\omega_P x_{\mathrm{PRJ},P}) \\ b_P \sin(\omega_P x_{\mathrm{PRJ},P}) \end{bmatrix}$$

$$\begin{bmatrix} \langle 1, 1\rangle & \langle 1, c_1\rangle & \langle 1, s_1\rangle & \ldots & \langle 1, c_P\rangle & \langle 1, s_P\rangle \\ \langle c_1, 1\rangle & \langle c_1, c_1\rangle & \langle c_1, s_1\rangle & \ldots & \langle c_1, c_P\rangle & \langle c_1, s_P\rangle \\ \langle s_1, 1\rangle & \langle s_1, c_1\rangle & \langle s_1, s_1\rangle & \ldots & \langle s_1, c_P\rangle & \langle s_1, s_P\rangle \\ \vdots & \vdots & \vdots & \ddots & \vdots & \vdots \\ \langle c_P, 1\rangle & \langle c_P, c_1\rangle & \langle c_P, s_1\rangle & \ldots & \langle c_1, c_P\rangle & \langle c_P, s_P\rangle \\ \langle s_P, 1\rangle & \langle s_P, c_1\rangle & \langle s_P, s_1\rangle & \ldots & \langle s_1, c_P\rangle & \langle s_P, s_P\rangle \end{bmatrix}$$

$$\mathbf{w} = \begin{bmatrix} w_0 \\ w_{c,1} \\ w_{s,1} \\ \vdots \\ w_{c,P} \\ w_{s,P} \end{bmatrix} = \mathbf{G}^{-1} \begin{bmatrix} \langle I_{\mathrm{CAM}}, 1\rangle \\ \langle I_{\mathrm{CAM}}, c_1\rangle \\ \langle I_{\mathrm{CAM}}, s_1\rangle \\ \vdots \\ \langle I_{\mathrm{CAM}}, c_P\rangle \\ \langle I_{\mathrm{CAM}}, s_P\rangle \end{bmatrix}$$

Signal decomposition for one camera

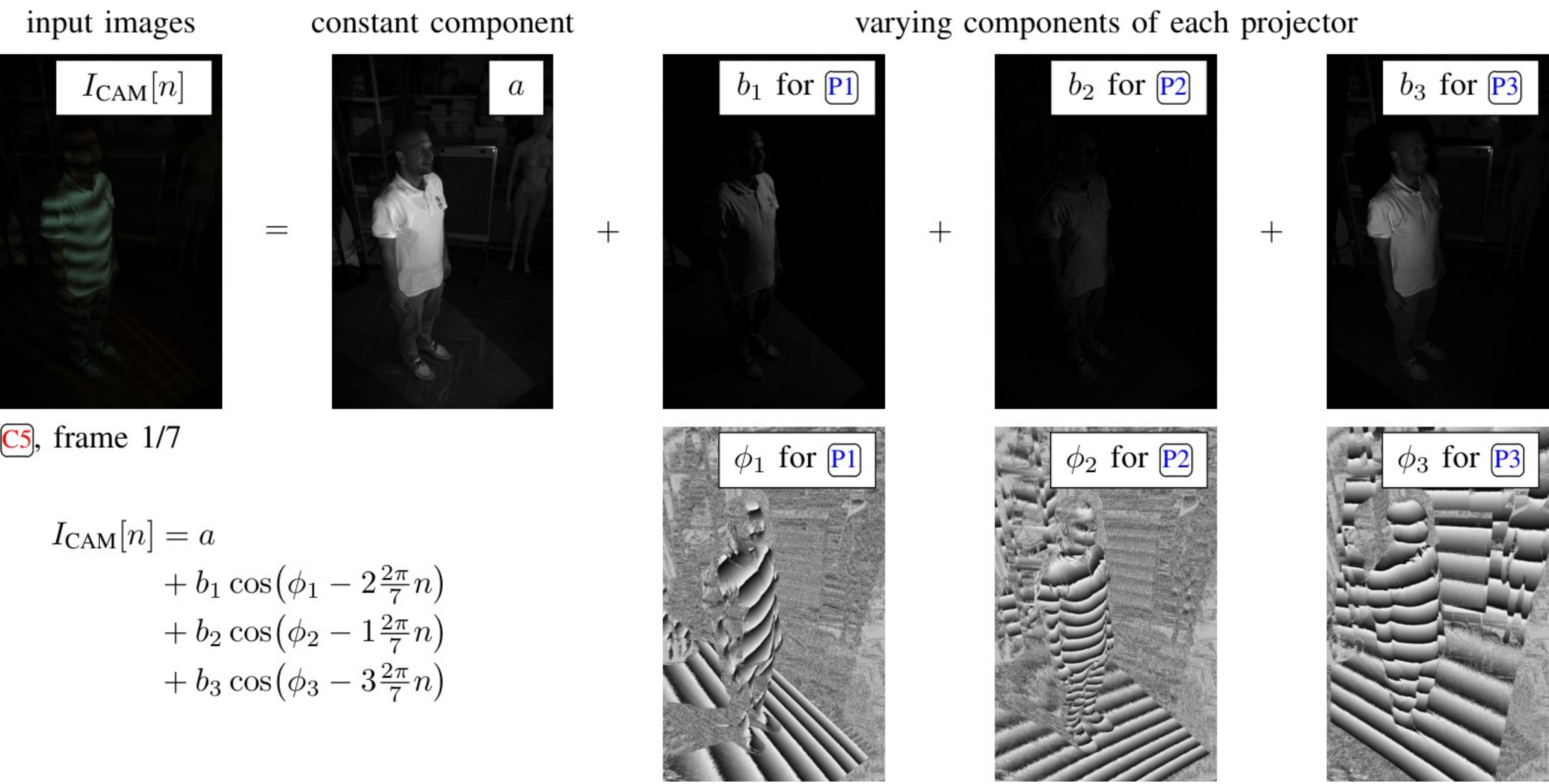

$$
\begin{aligned}
I_{\mathrm{CAM}}[n] = a \\
&+ b_1 \cos\left(\phi_1 - 2\tfrac{2\pi}{7}n\right) \\
&+ b_2 \cos\left(\phi_2 - 1\tfrac{2\pi}{7}n\right) \\
&+ b_3 \cos\left(\phi_3 - 3\tfrac{2\pi}{7}n\right)
\end{aligned}
$$

21 input frames in three groups of 7 frames are first decomposed into nine wrapped phases from which x_{PRJ} is computed.

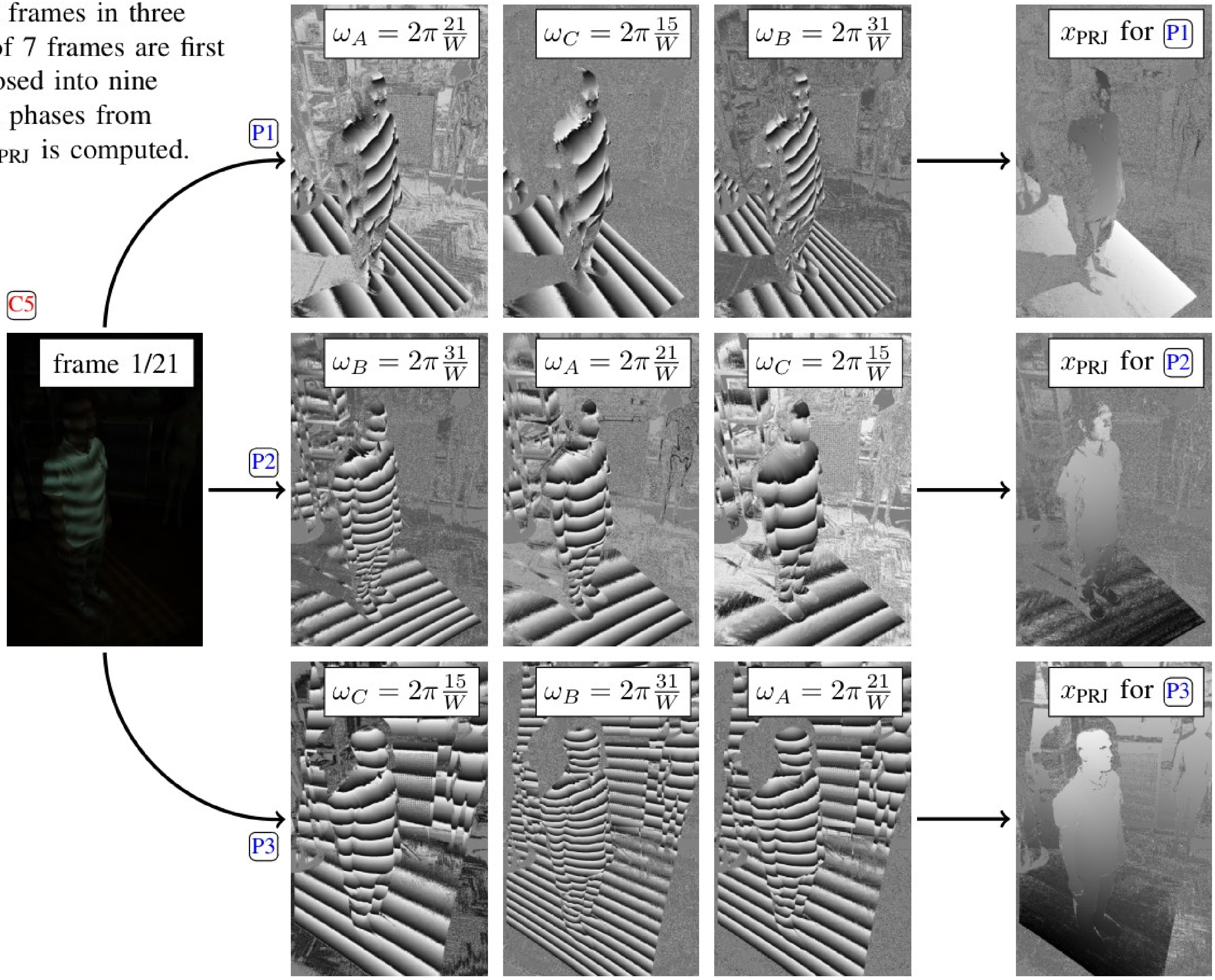

Example of multi-projector interference

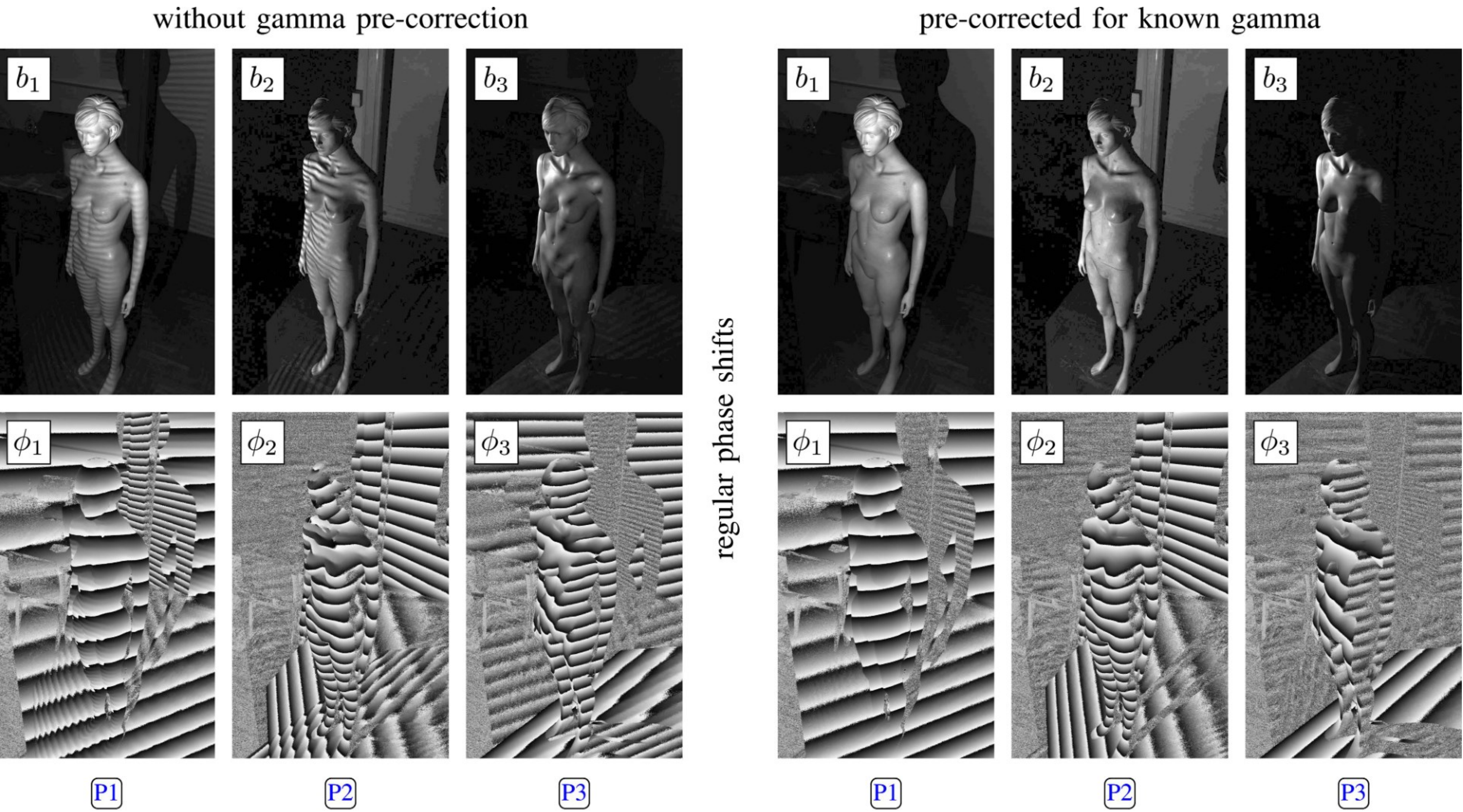

Calibration

- Both geometric and photometric calibration is required
- Geometric calibration
  - a double-sided calibration board
  - hexagonal circular pattern with side markers
  - transform between sides is know
- Photometric calibration
  - only gamma correction
  - can be omitted at the cost of a significant increase in the number of projected images

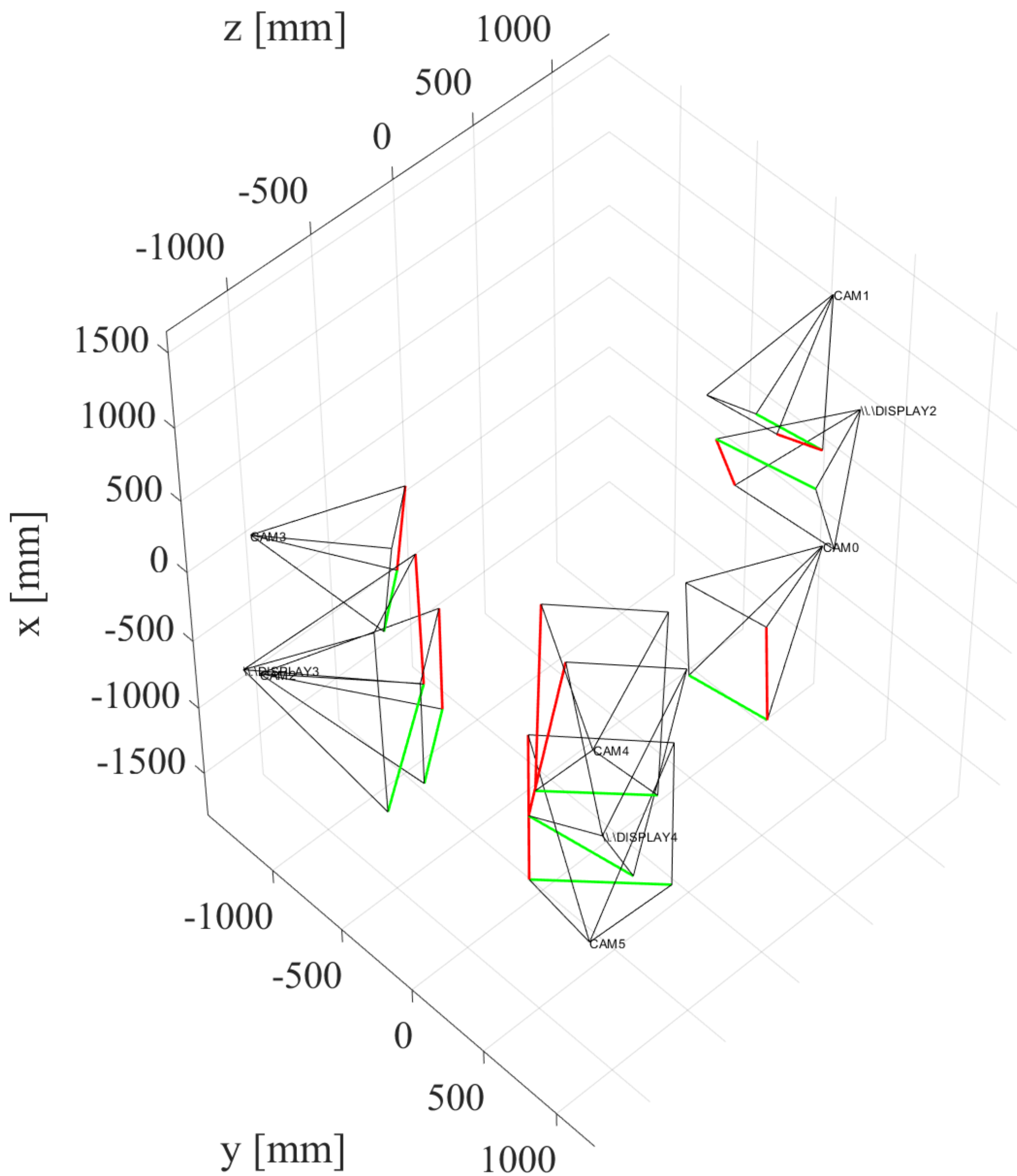

Calibration Objects

2D: calibration boards

1D: calibration wands

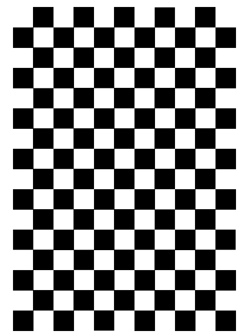

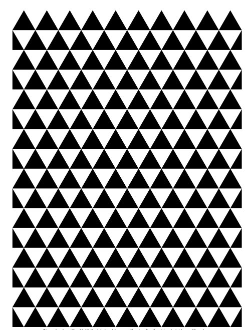

3D: calibration cages

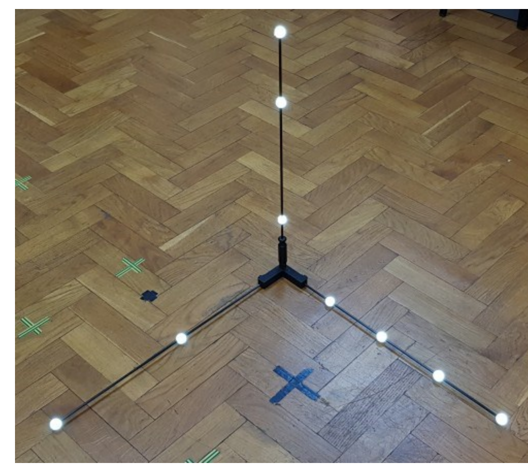

Pattern Processing

scale-space detection of circles

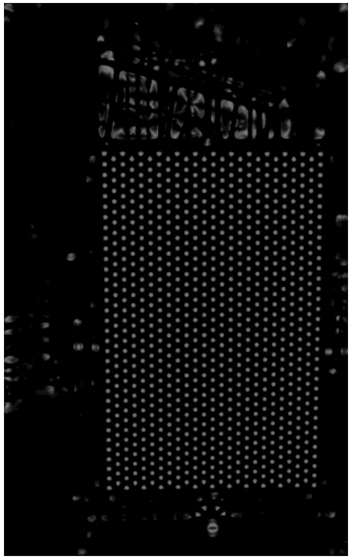

circle center detection with non-maximum suppression

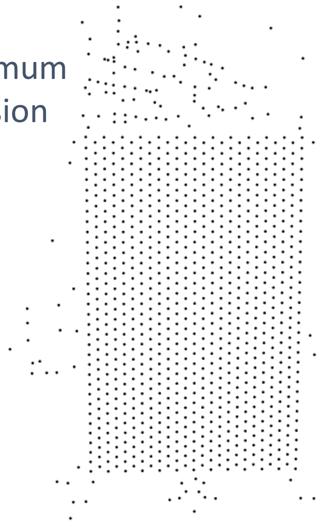

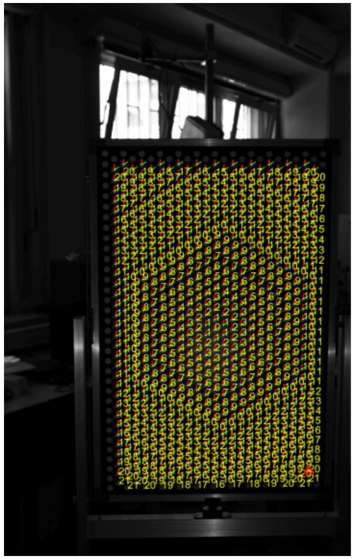

Extracted Grids

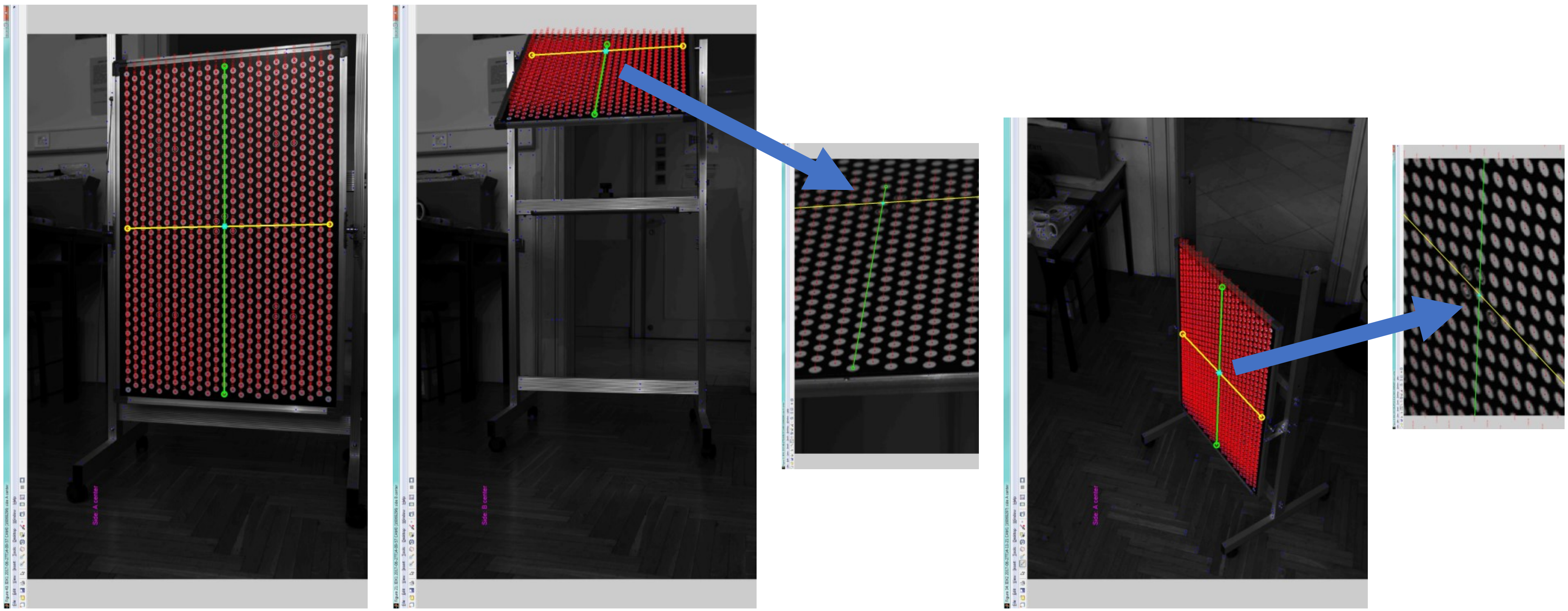

Colorimetric Calibration

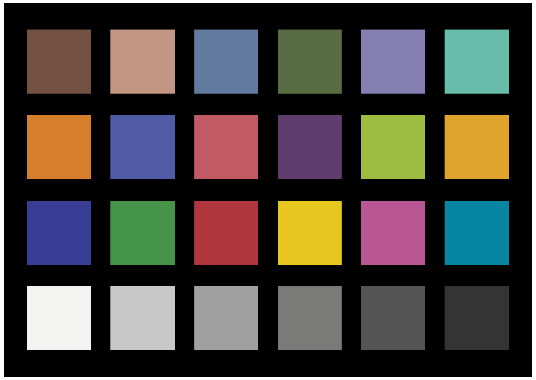

standard colorimetric
calibration board

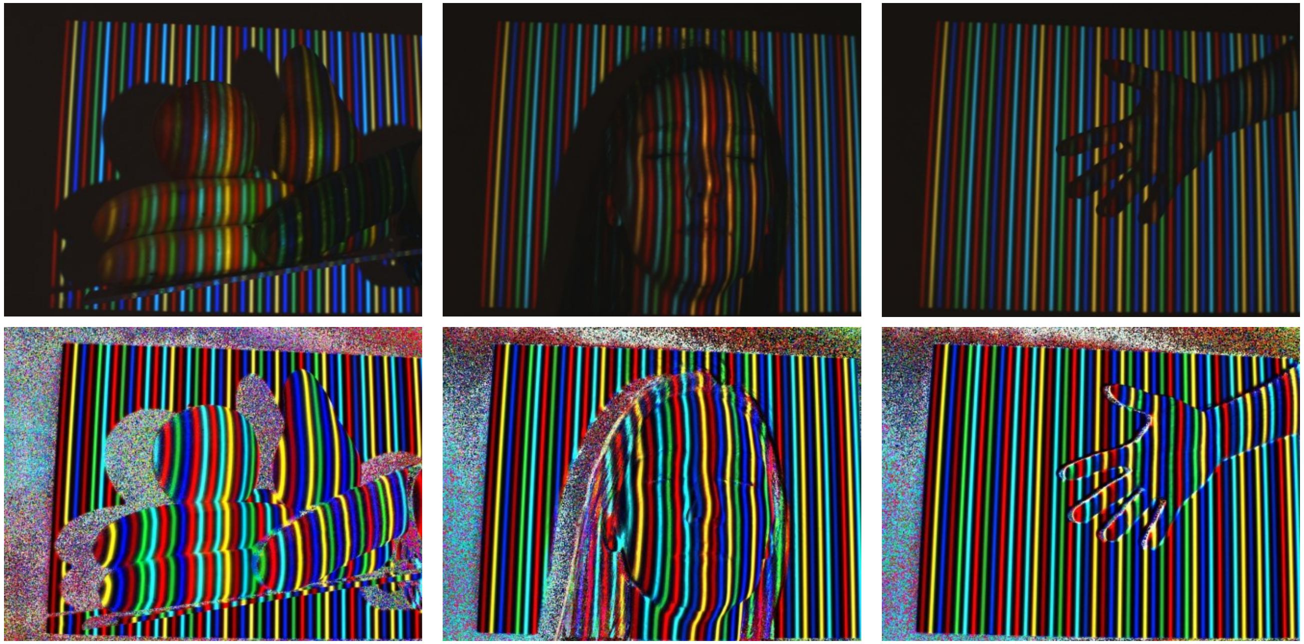

Selection of phase shifts and of spatial frequencies

- Phase shifts $\varphi_p[n]$ must be selected so the system of equations is solvable
- There exists a convenient selection of phase shifts which enables efficient decomposition via FFT

$$\Omega_p = 2p\pi/(2P+1), \quad p = 1, \ldots, P$$
$$\varphi_p[n] = \Omega_p(n-1), \quad n = 1, \ldots, 2P+1$$

- Spatial frequencies $\omega_p[n]$ must be selected so the system of equations is solvable
- At least two frequencies are required per projector to enable reliable phase unwrapping via Chinese reminder theorem
- Higher frequencies are preferable due to better properties

Example:
three spatial frequencies and phase unwrapping

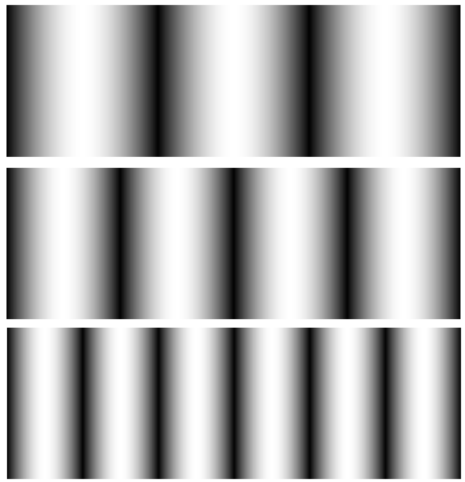

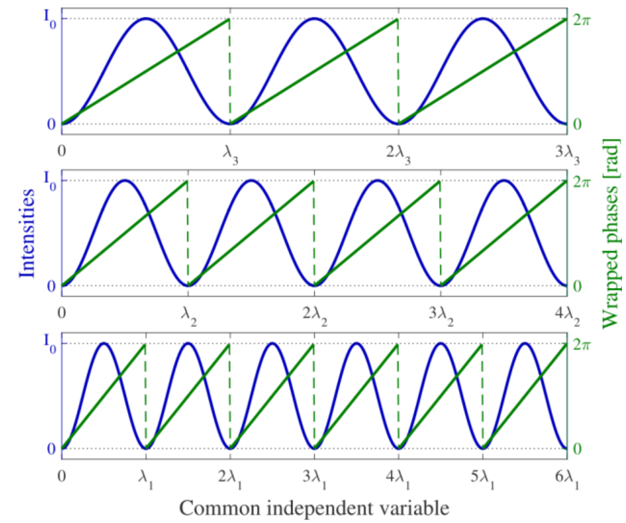

To unwrap the phase the following system of equations must be solved:

$$\Phi_1 = \phi_1 + 2\pi k_1$$

$$\Phi_2 = \phi_2 + 2\pi k_2$$

$$\Phi_3 = \phi_3 + 2\pi k_3$$

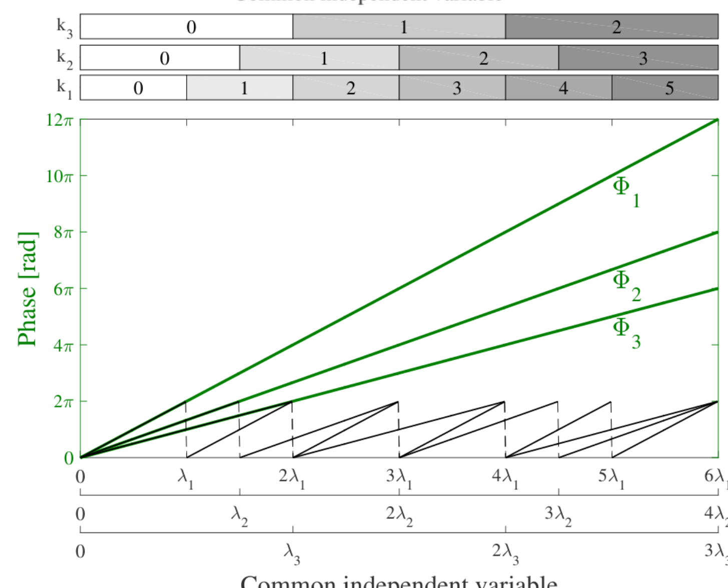

Two frequency example

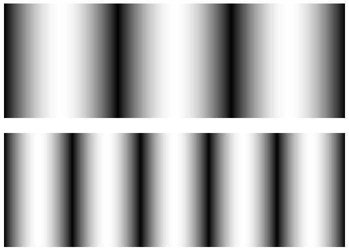

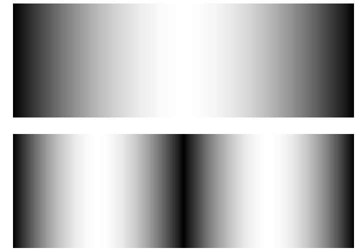

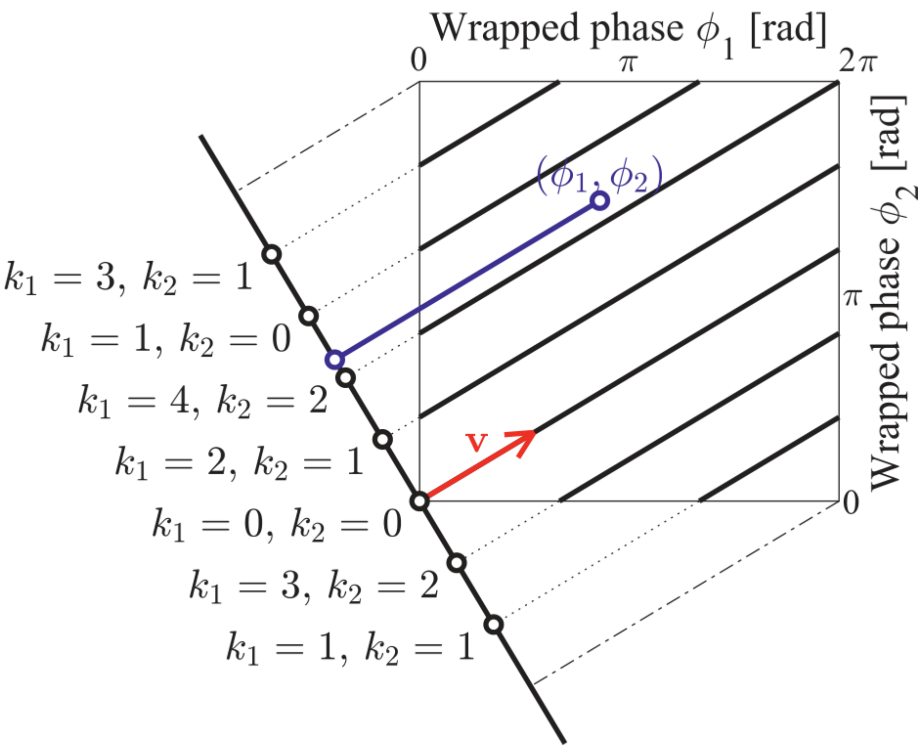

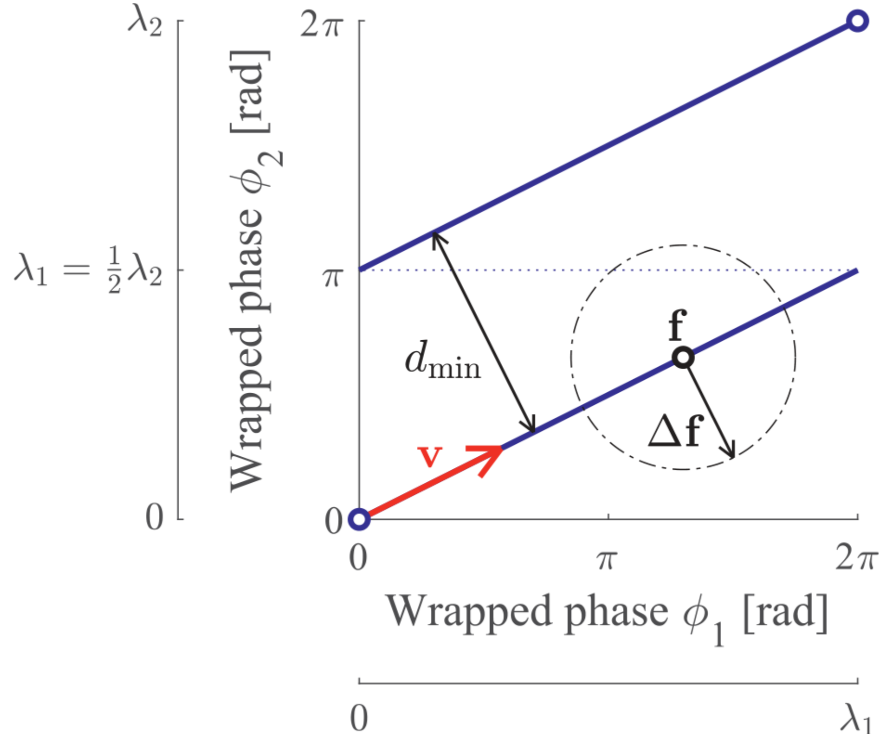

Optimal frequency selection

- Optimality is defined w.r.t. the noise robustness to phase unwrapping
- Optimization is not differentiable
  - Exhaustive search (cannot use gradient descent)
- Instead of spatial frequencies it is more convenient to search over the fringe counts
- The projector coordinate x_{PRJ} is limited to $0 < x_{PRJ} < X$ interval (normalized, not measured in px). Let N_i be the fringe count for the wavelength λ_i. Then:

$$X = \mathrm{LCM}(\lambda_1, \ldots, \lambda_M) \qquad N_m = \frac{\mathrm{LCM}(\lambda_1, \ldots, \lambda_M)}{\lambda_m} = X f_m$$

$$\lambda_1 N_1 = \cdots = \lambda_m N_m = \cdots = \lambda_M N_M = X$$

$$X = \mathrm{LCM}(\lambda_1, \ldots, \lambda_M) = \mathrm{LCM}(N_1, \ldots, N_M)$$

$$\lambda_m = \frac{X}{N_m} = \frac{\mathrm{LCM}(N_1, \ldots, N_M)}{N_m}$$

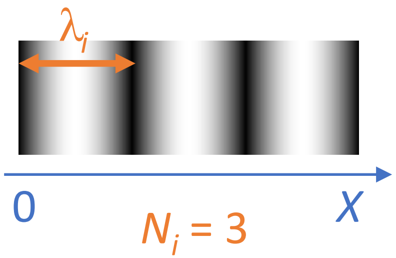

Exhaustive Search Over Viable Fringe Counts

- Exhaustive search is performed over viable fringe counts
- We select minimal and maximal number of fringe counts over the whole projector width (or height)
- Search complexity is factorial, but for regularly used fringe counts the total search time is acceptable

M	$N_{\min}$	$N_{\max}$	Runtime
2	40	80	0.2 seconds
	50	100	0.3 seconds
3	40	80	2.6 seconds
	50	100	7.0 seconds
4	40	80	42.2 seconds
	50	100	2.3 minutes
5	40	80	7.9 minutes
	50	100	32 minutes
6	40	80	67 minutes
	50	100	5.9 hours

Selecting optimal spatial frequencies w.r.t. resistance to wrapped phase noise

Table 2
The best and the worst selection of fringe counts for [40,80] interval. Intended for encoding projector rows.

M	Counts in [40,80]	*d* [deg]	*d* [rad]
2	40:41	3.14°	0.055
	79:80	1.60°	0.028
3	40:41:52	21.95°	0.383
	78:79:80	3.22°	0.056
4	42:43:46:56	42.36°	0.739
	77:78:79:80	5.13°	0.090
5	43:47:49:54:68	61.16°	1.067
	76:77:78:79:80	7.30°	0.127
6	40:41:44:46:54:66	78.81°	1.376
	75:76:77:78:79:80	9.71°	0.170

Table 3
The best and the worst selection of fringe counts for [50,100] interval. Intended for encoding projector rows.

M	Counts in [50,100]	*d* [deg]	*d* [rad]
2	50:51	2.52°	0.044
	99:100	1.28°	0.022
3	50:57:58	18.95°	0.331
	98:99:100	2.57°	0.045
4	52:53:56:68	39.86°	0.696
	97:98:99:100	4.09°	0.071
5	50:56:57:65:76	58.27°	1.017
	96:97:98:99:100	5.81°	0.101
6	51:52:60:64:78:80	73.85°	1.289
	95:96:97:98:99:100	7.72°	0.135

Table 4
The best and the worst selection of fringe counts for [64,128] interval. Intended for encoding projector columns.

M	Counts in [64,128]	*d* [deg]	*d* [rad]
2	64:65	1.97°	0.034
	127:128	1.00°	0.017
3	64:65:73	17.50°	0.305
	126:127:128	2.00°	0.035
4	64:68:73:84	37.15°	0.648
	125:126:127:128	3.18°	0.056
5	66:67:72:75:96	54.49°	0.9511
	124:125:126:127:128	4.52°	0.079
6	65:66:71:78:81:113	71.29°	1.2442
	123:124:125:126:127:128	6.00°	0.105

Table 5
The best and the worst selection of fringe counts for [80,160] interval. Intended for encoding projector columns.

M	Counts in [80,160]	*d* [deg]	*d* [rad]
2	80:81	1.58°	0.028
	159:160	0.80°	0.014
3	80:82:97	15.77°	0.275
	158:159:160	1.60°	0.028
4	80:81:85:101	34.34°	0.599
	157:158:159:160	2.54°	0.044
5	80:81:84:109:127	52.42°	0.915
	156:157:158:159:160	3.60°	0.063
6	80:81:83:89:107:120	69.44°	1.212
	155:156:157:158:159:160	4.78°	0.083

Is there an optimal number of frequencies?

- Under the assumption of independence between wrapped phase measurements expected deviation is

$$\Delta \mathbf{f}^2 = \sigma_1^2 + \sigma_2^2 + \cdots \sigma_m^2 + \cdots + \sigma_M^2$$

- For M spatial frequencies and the minimal half-distance d we have an upper limit

$$\sigma < \frac{d}{\sqrt{M}}$$

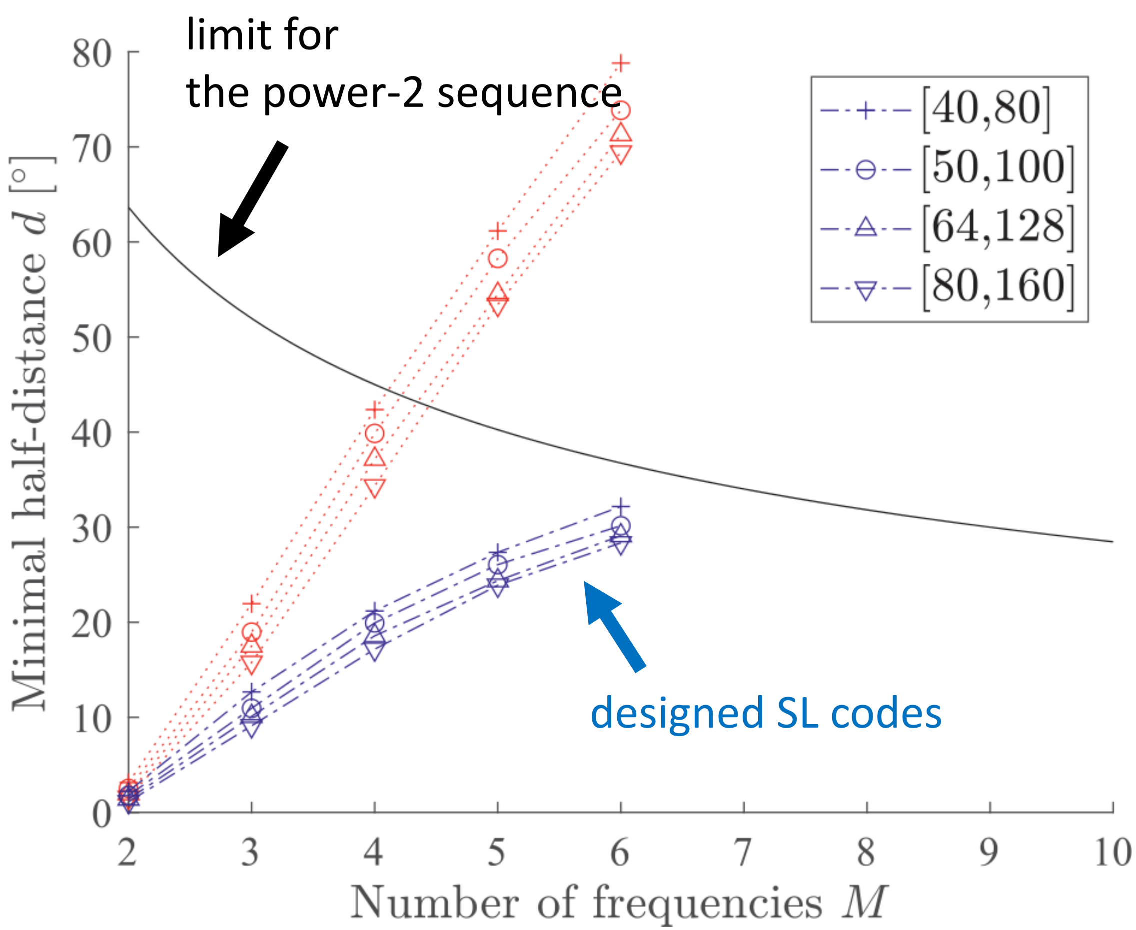

Point cloud filtering

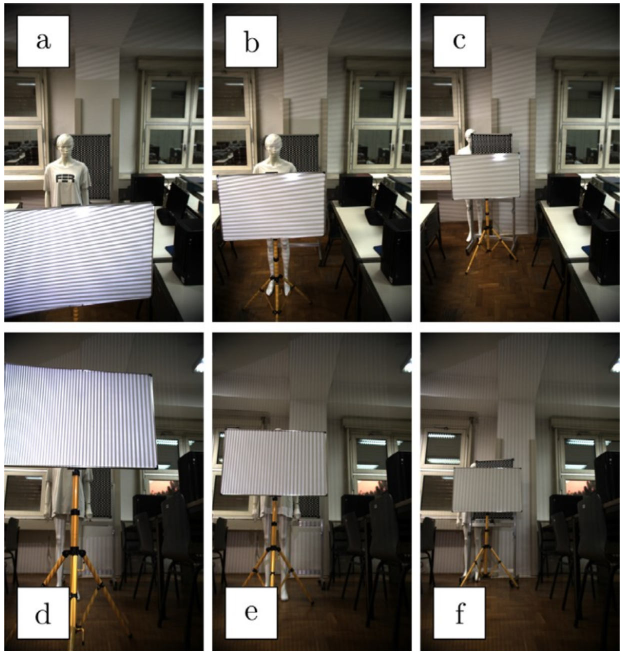

- Filter out all points which are farther from the line-constellation then some predefined threshold

$$\Delta \mathbf{f} < d_{\text{thr}} = k \cdot d_{\text{min}}, \quad 0 < k < 1$$

Underwater imaging and physical properties of water

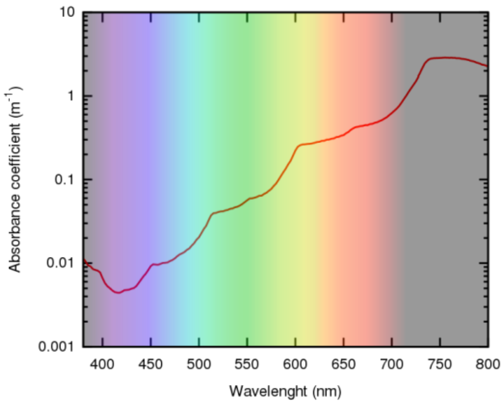

(source of images: Wikipedia)

- Liquid water strongly absorbs electromagnetic radiation
- There is a narrow window of weak absorption
  - it includes the visible spectrum
  - the lowest absorption is for the blue light (at 418 nm for water at 22°C)
- Underwater imaging using the visible spectrum is of particular interest
- Compared to ultrasound imaging
  - spatial resolution is better when using visible light
  - imaging range/distance is better when using sound

Challenges of underwater imaging

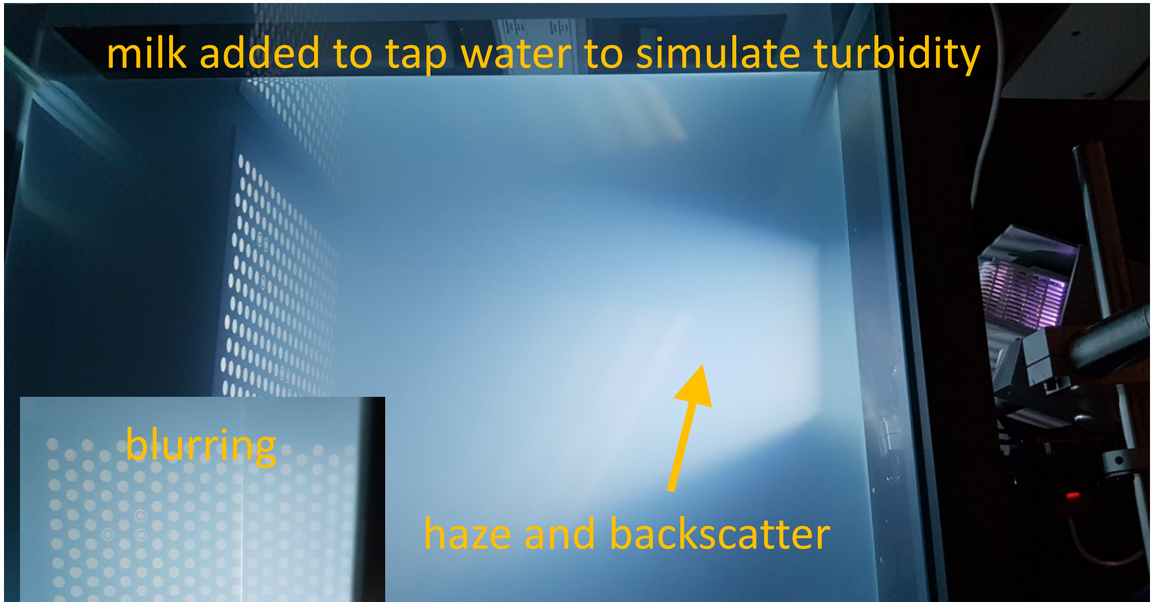

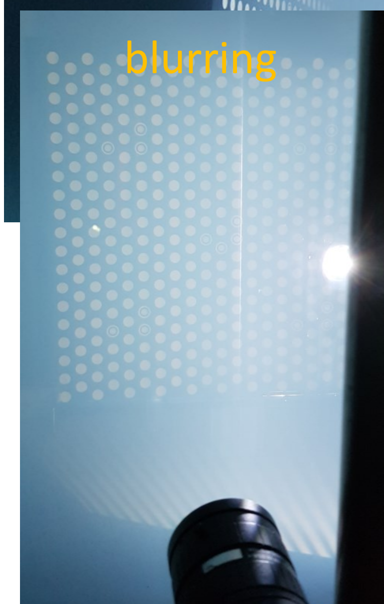

- Compared to in-the-air imaging
  - the absorption coefficient of liquid water is much higher
  - turbidity of water causes blurring, haze, and backscatter
  - air-to-water interface causes refractions

Key prerequisites for successful imaging

- Well designed structured light patterns to be projected
  - most often a set of moving sinusoidal fringes, selection of spatial shape is difficult
- A comprehensive image formation model
  - should account for refractions, backscatter and blurring
- A robust and easy to use calibration procedure
  - calibrate on land/in the laboratory, minimal adjustments in the field
- A practical underwater enclosure for imaging equipment
  - allows adjustments to set the baseline and overlapping fields of view

Structured light patterns

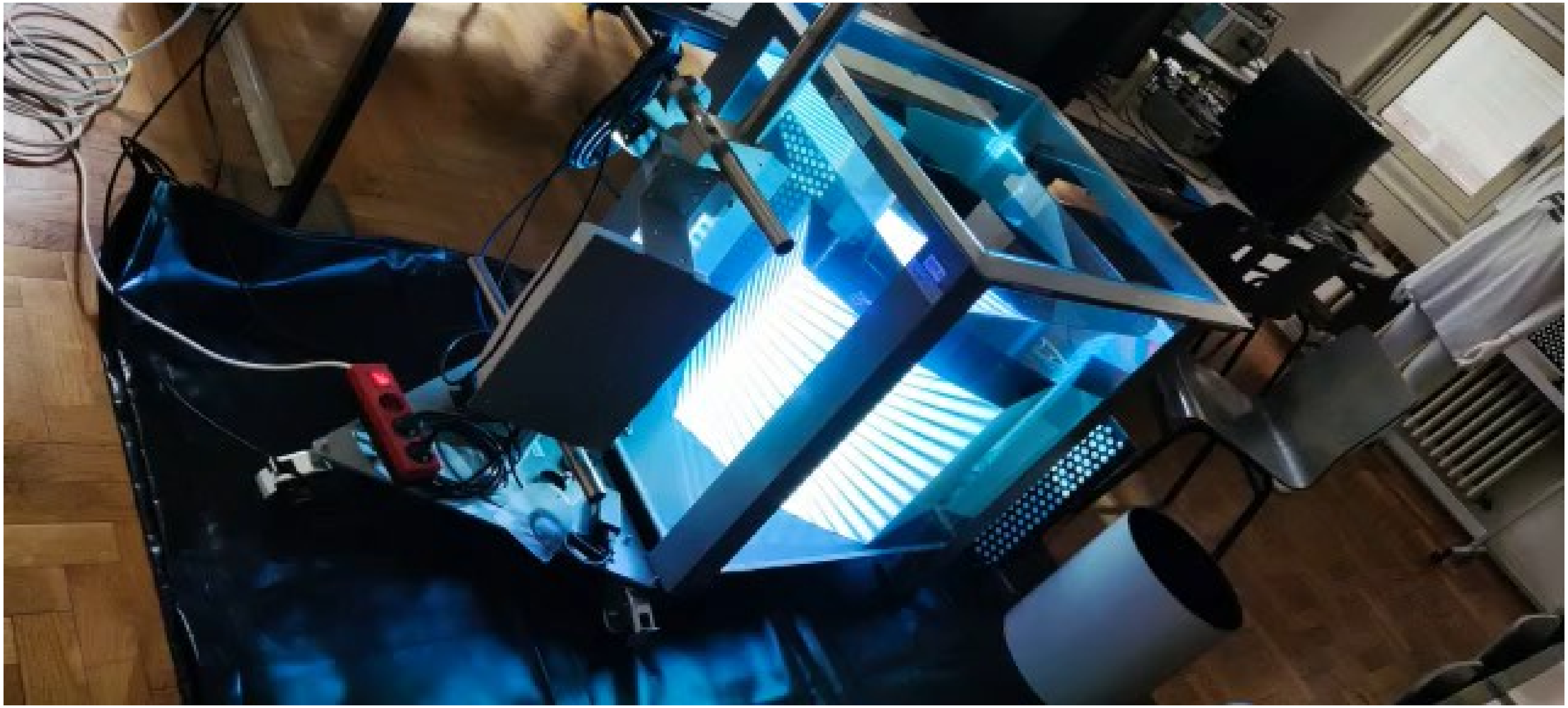

- A sinusoidal fringe with varying phase shifts, spatial frequencies and orientations is projected.

Image formation model

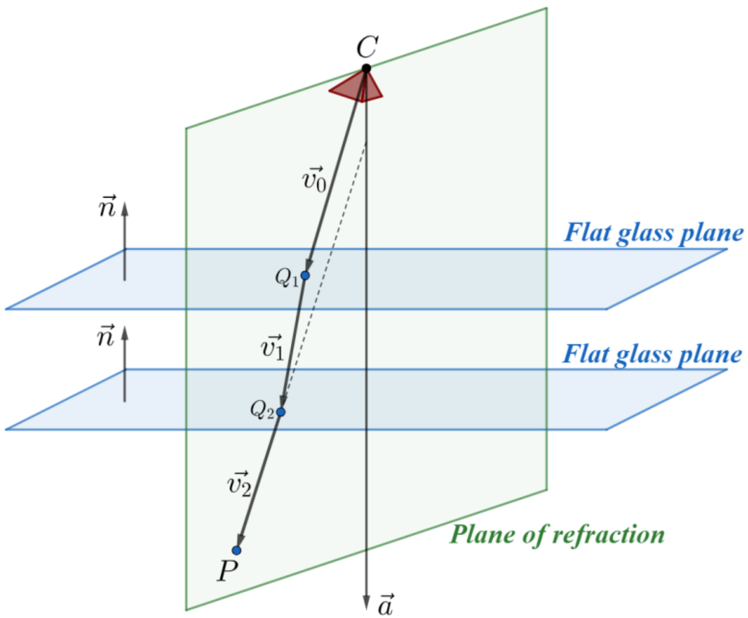

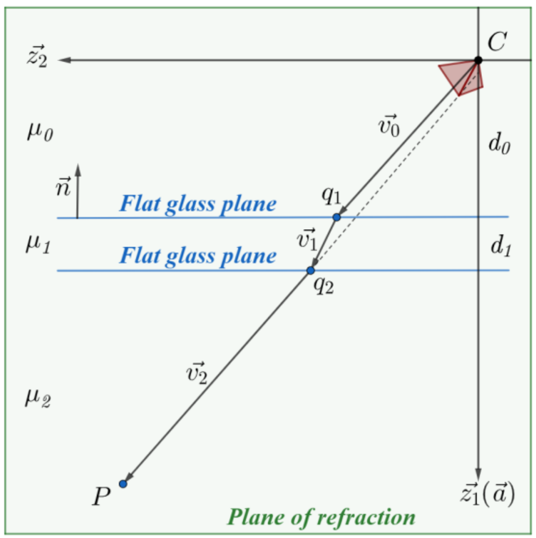

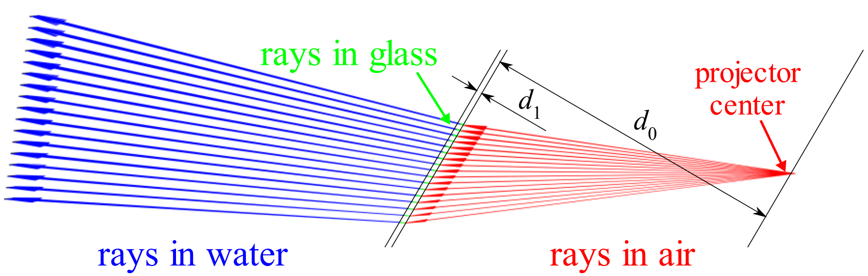

- Developed for flat refractive interfaces
  - a flat acrylic sheet is a viewport for camera to image and for projector to illuminate
  - a key concept is plane-of-refraction
  - it is similar to an axial camera model

Calibration procedure

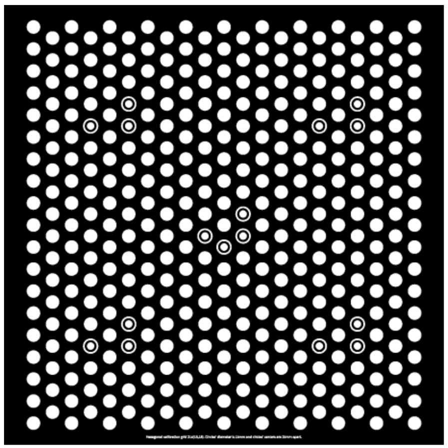

flat calibration board

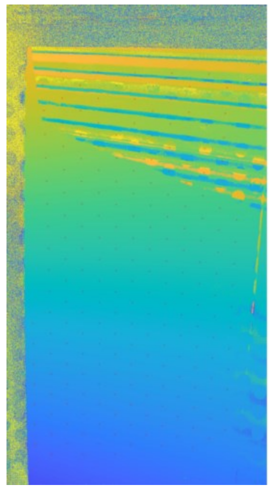

projector columns

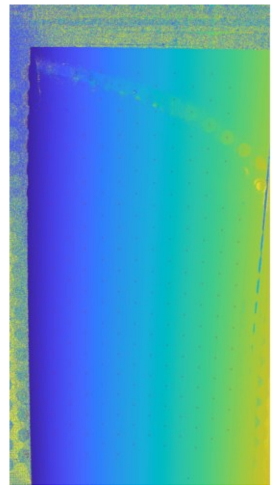

projector rows

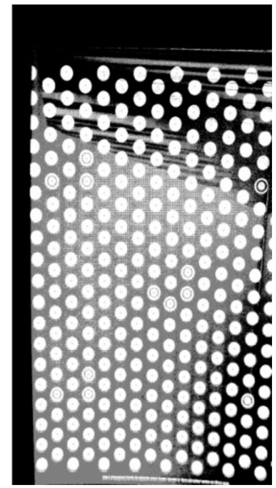

illuminated area

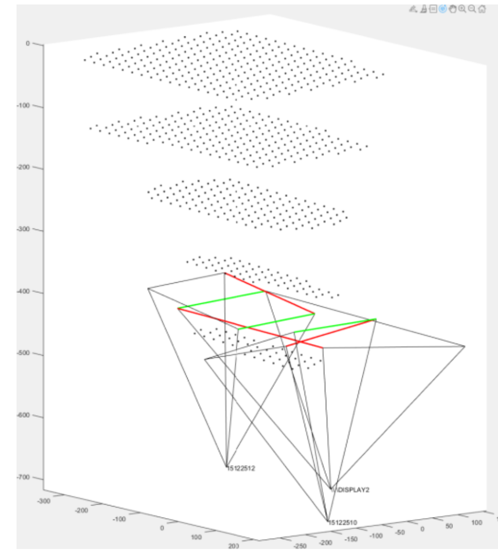

imaging geometry

- Calibration can be performed in the laboratory
- Imaging is possible both in air and underwater simply by changing the refraction index of the last medium

Prototype of an underwater SL scanner

two cameras
(image
acquisition)

one projector
(illumination)

three watertight
enclosures
and support
structure

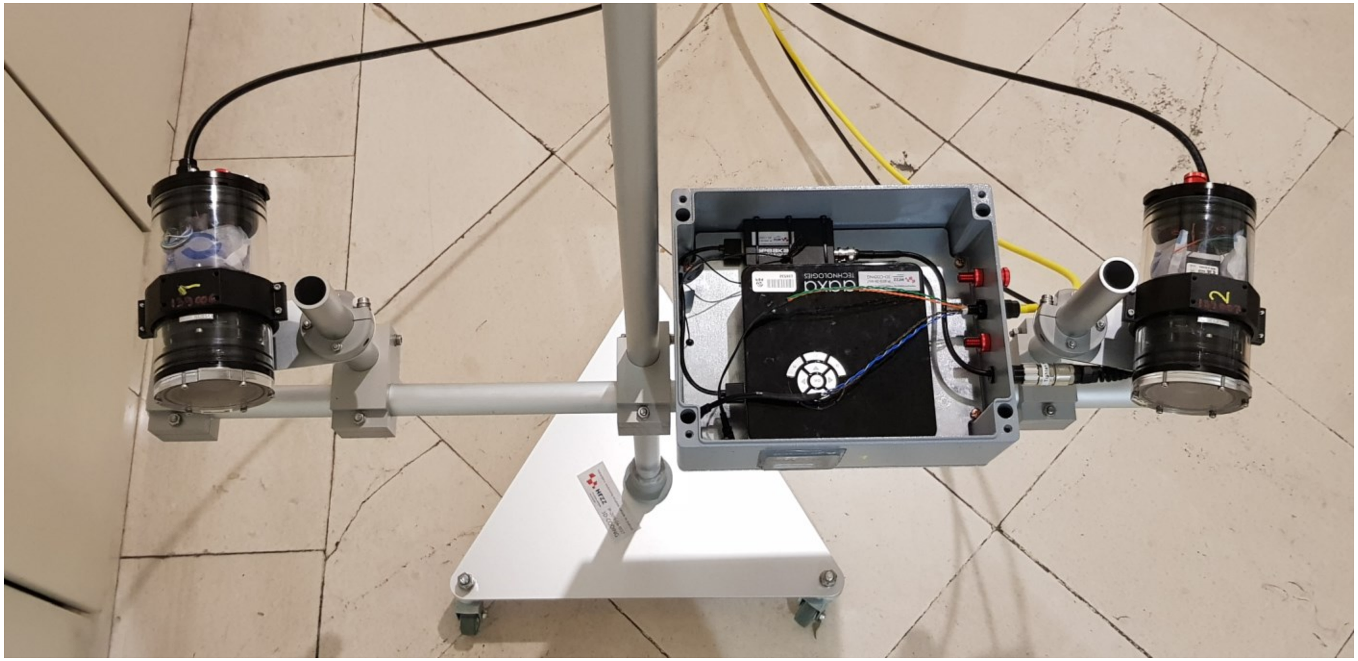

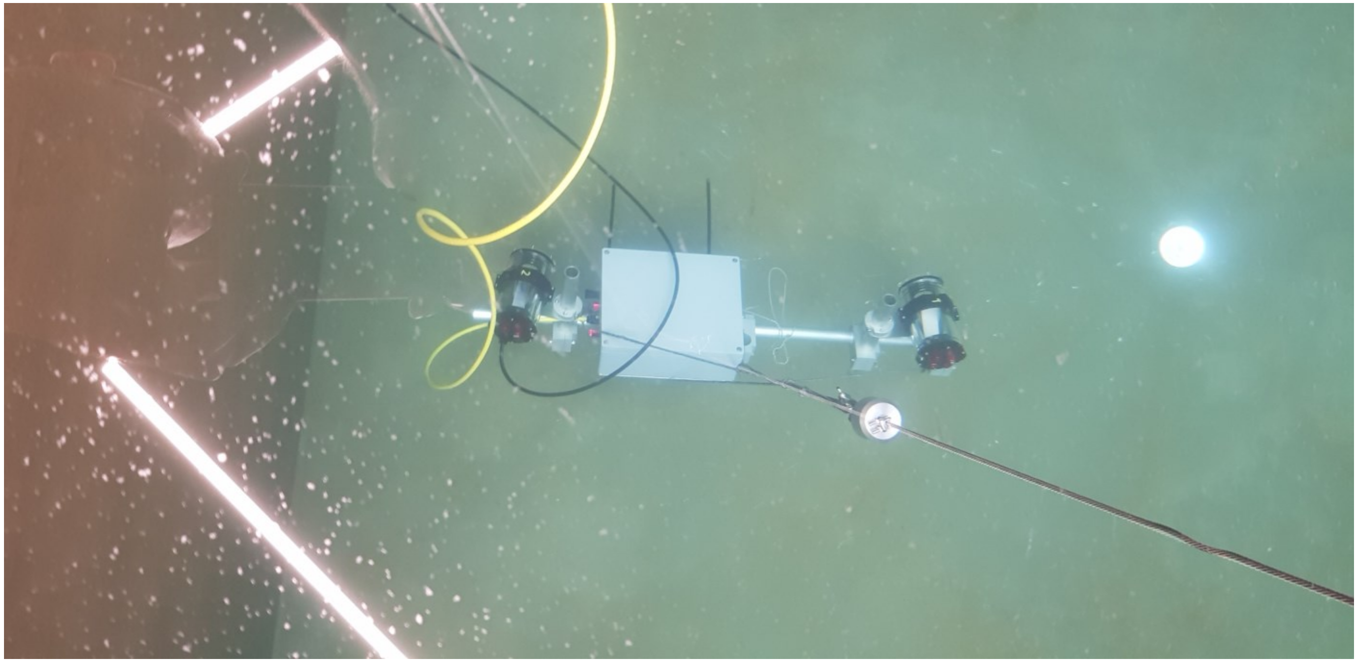

Verification via known objects

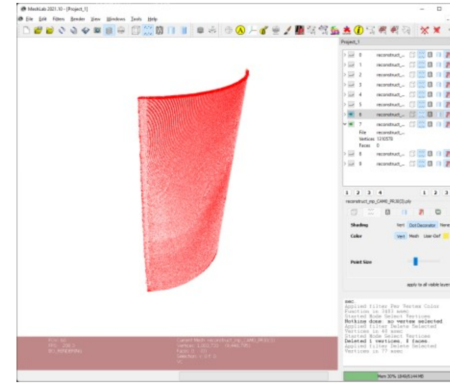

Two verification objects are a cube and a cylinder of known dimensions.

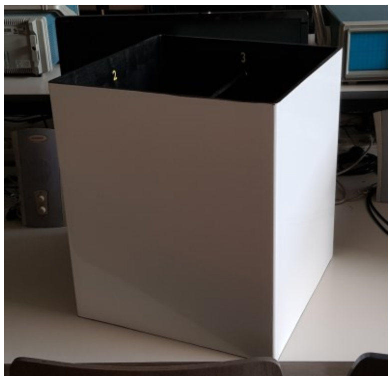

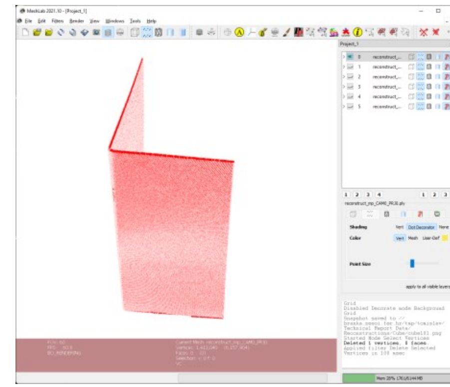

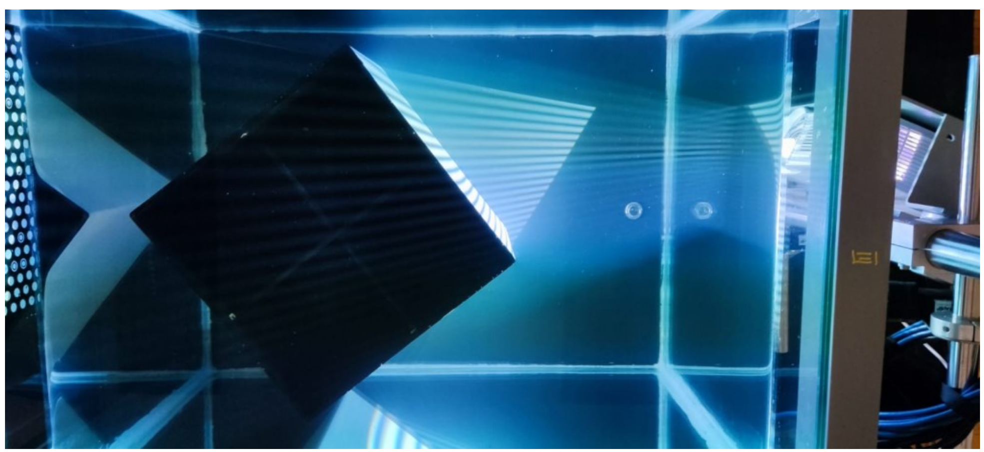

3D scanning in clear water

3D reconstruction

Conclusion and future work

- Considerations when designing a structured light 3D system
  - optical setup – surrounding the object with sensors or moving the object in front of a sensor
  - structured light pattern – scanning time vs. resolution vs. robustness
  - fringe projection profilometry – we have a good understanding of how to select all relevant parameters of the structured light imaging system

- Future work
  - designing spatially pre-warped structured light patterns which are insensitive to flat refractive interface
  - research Fourier imaging to measure the light transportation matrix and enable imaging under very high turbidity
  - investigate possibilities of spatio-temporal processing to enable imaging dynamic scenes

References

1. Petković, Tomislav; Pribanić, Tomislav. "**Multi-Projector Multi-Camera Structured Light Surface Scanner.**" IEEE Access, Vol. 10, 2022, pp. 90321-90337, https://doi.org/10.1109/ACCESS.2022.3200388
2. Petković, Tomislav; Pribanić, Tomislav; Zoraja, Domagoj. "**Selection of optimal frequencies in multiple-frequency fringe projection profilometry.**" Optics and lasers in engineering, Vol. 163, 2023, https://doi.org/10.1016/j.optlaseng.2022.107455
3. Zoraja, Domagoj; Petković, Tomislav; Forest, Josep; Pribanić, Tomislav. "**Calibration of a Structured Light Imaging System in Two-Layer Flat Refractive Geometry for Underwater Imaging**". Sensors, Vol. 23(12), https://doi.org/10.3390/s23125444
4. Petković, Tomislav; Pribanić, Tomislav; Đonlić, Matea. "**Temporal phase unwrapping using orthographic projection.**" Optics and lasers in engineering. 90 (2017), 34-47, https://doi.org/10.1016/j.optlaseng.2016.09.006
5. Petković, Tomislav; Gasparini, Simone; Pribanić, Tomislav. "**A Note on Geometric Calibration of Multiple Cameras and Projectors**." 2020 43rd International Convention on Information, Communication and Electronic Technology (MIPRO), Opatija, Croatia, 2020, pp. 1157-1162, https://doi.org/10.23919/MIPRO48935.2020.9245316.
6. Zoraja, Domagoj; Petković, Tomislav; Pribanić, Tomislav; Forest, Josep. "**Projector Calibration in a Two-Layer Flat Refractive Geometry for Underwater Imaging**" 2022 45th International Convention on Information, Communication and Electronic Technology (MIPRO), Opatija, Croatia, 2022, https://doi.org/10.23919/MIPRO55190.2022.9803454
7. Puljčan, Ana; Zoraja, Domagoj; Petković, Tomislav. "**Simulation of Structured Light 3D Scanning using Blender.**" 64th International Symposium ELMAR-2022, Zadar, Croatia, 2022, https://doi.org/10.1109/ELMAR55880.2022.9899809